コンクリート工学論文集 第9巻第2号 1998年7月

Multiple Cracking Sequence and Saturation in Fiber Reinforced Cementitious Composites

Tetsushi Kanda[1] and Victor C. Li[2]

Synopsis : This study has aimed at clarifying the sequence and saturation of multiple cracking evolution in Random Short Fiber Reinforced Cementitious Composites with Pseudo Strain Hardening Behavior (PSH-RSFRCCs). For this purpose, uniaxial tensile tests were conducted with Polyethylene fiber composites. Unsaturated multiple crack evolution was observed as well as saturated evolution in these tests depending on fiber volume fraction and testing age. Plausible mechanisms were suggested to characterize these two crack evolution types. Furthermore, two micromechanics based performance indices were proposed as measures of crack saturation.

Keywords : fiber reinforced cementitious composite, micromechanics, pseudo strain hardening

1. INTRODUCTION

Micromechanical composite design methodology has led to the development of extremely ductile cementitious composites with moderate fiber content in recent years. For example one such composite reinforced with 2 volume percent random short polyethylene fibers exhibits over 5% tensile strain capacity (e.g., [1]). This remarkably high strain capacity is a result of numerous fine cracks developed perpendicular to the loading axis with small crack spacing (around 2 mm for the Polyethylene composites [2] at fully saturated state) in uniaxial tensile tests. These composites show clear bilinear stress-strain curves with a bend-over point at first cracking before eventually attaining peak stress, after much extensive inelastic straining beyond first crack. This king of stress-strain relation is referred to as Pseudo Strain Hardening (PSH) behavior, and such property as in the Polyethylene fiber composite is specifically referred to as "saturated PSH" in this article. The micromechanical composite design methodology has been investigated in detail (e.g., [3] and [4]), providing design criteria in terms of required combination of the magnitudes of micromechanical parameters such as bond strength and fiber aspect ratio. These design criteria have been validated for saturated PSH-RSFRCCs (Random Short Fiber Reinforced Cementitious Composites) with reasonable accuracy [5].

Recent more detailed experimental observations suggest that the assumptions behind the theoretical treatment of the multiple cracking phenomena may not be fully satisfied in certain composites. For example, even in the case of saturated PSH materials, multiple cracking evolves as a function of increasing applied load, rather than an immediate spread from first crack to full saturation at the first crack stress [2]. In addition, it has been observed that the first crack (or the last crack) may not be the same as the failure crack which opens up with descending load when deformation localization is realized at ultimate stress. Finally, in some composites, a state somewhere between brittle single cracking and fully saturated multiple cracking, here referred to as unsaturated multiple cracking, or "unsaturated PSH", occurs. This study defines the saturated PSH as the phe-

1 Graduate student, Dept. of Civil and Envir. Eng., University of Michigan, USA (on leave from Kajima Technical Research Institute), Member of JCI

2 Professor and Director, ACE-MRL, Dept. of Civil and Envir. Eng., University of Michigan, USA

nomenon in which crack spacing depends on distance necessary to transfer fiber stress at crack plane to matrix via interface friction. On the other hand, the unsaturated PSH is observed when crack spacing is never reduced to the necessary distance.

This paper documents the above phenomena, and suggests extensions of the current theoretical treatment in order to account for these observations. Specifically we report on experimental observations of stress-strain relations, crack spacing, and crack openings in composites which varied in fiber volume fraction and test age. The fiber volume fraction and test age have been used as means to control the bridging properties of fibers across matrix cracks, and the matrix toughness, respectively. These factors directly influence the maximum fiber bridging stress of a composite and the first crack strength. Consideration of the variation of these factors, as well as the complementary bridging energy [6, 3, 7], in the context of the First Crack Strength Criterion and the Steady State Cracking Criterion proposed by Li [4] for multiple cracking, leads to two proposed theoretical indices which should approximate the degree of multiple crack saturation.

PSH-RSFRCCs, or ECCs (Engineered Cementitious Composites), are being investigated for structural applications [8 and 9]. In all of these application studies the composite tensile strain capacity, governed by the degree of PSH saturation, is exploited for enhancing structural performance. The ultimate purpose of this study is to establish design guidelines for controlling the tensile strain capacity of ECCs by adopting the micromechanics approach. As well, this study should contribute to a wider range of materials (especially fibers) suitable for the development of ECCs.

In the following a brief review of some fundamental mechanics of pseudo strain-hardening is presented. Section 2 serves to provide the context for design of the experiments (Section 3), and the theoretical basis for interpretation (Section 5) of the experimental results (Section 4).

2. FUNDAMENTAL MECHANICS

2.1 Criteria For Multiple Cracking

The presence or absence of multiple cracking or PSH under uniaxial tension for RSFRCCs is governed by a pair of complementary criteria: a) First Crack Stress Criterion and b) the Steady State Cracking Criterion [4 and 7]. If either of these criteria is not satisfied, no multiple cracking can exist, and the material fails with a single crack.

a) First Crack Stress (FCS) Criterion

The First Crack Stress Criterion requires that the tensile stress at first crack must not exceed the maximum bridging stress available from fiber bridging of a matrix crack. If this criterion is not satisfied, immediate stress drop will accompany the first crack with bridging fibers being pulled out or ruptured. This first crack will continue to open with no new cracks created. This is the common behavior of brittle or quasi-brittle fiber reinforced brittle matrix composites.

The first crack stress is highly sensitive to the matrix flaw size and matrix toughness. It decreases approximately with the square-root of the flaw size when the flaw size is small, as in the case of a Griffith crack. An estimation of the magnitude of first crack strength in terms of matrix toughness K_{tip} and flaw size "c", and accounting for fiber bridging of a penny shape crack, is given in [4].

$$\hat{\sigma}_{fc}=g\left[\left(\frac{2\sqrt{2}}{3}\sqrt{\bar{c}}-\frac{\bar{c}}{4}\right)+\frac{\sqrt{\pi}}{2}\frac{\overline{K}}{\bar{c}}\right] \qquad (1)$$

where,

$$\hat{\sigma}_{fc}=\frac{\sigma_{fc}}{\sigma_0},\ \sigma_0=\frac{V_f\tau_i}{2}\left(\frac{L_f}{d_f}\right),\ g=\frac{2}{4+f^2}(1+e^{\pi f/2}),$$

$$\bar{c}=\frac{\sqrt{\hat{c}}}{\hat{\delta}^*},\ \hat{c}=\frac{c}{c_0},\ \hat{\delta}^*=\frac{2\tau_i}{E_f(1+\eta)}\frac{L_f}{d_f}$$

$$\eta=\frac{V_fE_f}{V_mE_m},\ \overline{K}=\frac{K_{tip}}{\sigma_0\sqrt{c_0}}\frac{1}{g\hat{\delta}^*},\ K_{tip}=K_m\left(\frac{E_c}{E_m}\right),$$

$$c_0=\left(\frac{L_fE_c}{2K_{tip}}\right)^2\frac{\pi}{16(1-\nu^2)^2}$$

f=Snubbing coefficient
τ_i=Frictional bond strength
V_f=Fiber volume fraction
E_f=Fiber elastic modulus
V_m=Matrix volume fraction
E_m=Matrix elastic modulus
L_f=Fiber length
d_f=Fiber diameter

c=crack radius

K_m=Matrix fracture toughness

E_c=Elastic modulus of composite

ν=Poisson's ratio of composite

Eqn. (1) has been derived from consideration of the net stress intensity factor due to applied loading and fiber bridging. Notice that this formula was obtained by slightly modifying the assumption of crack profile, in which half-parabola shape $\hat{\delta}=\frac{1}{2}\sqrt{\hat{c}\{1-(r/c)^2\}}$ (r=distance from crack center) was used instead of parabola shape in the original theory [4]. This modification has been recently found to increase the accuracy of σ_{fc} prediction [10].

The maximum crack bridging stress σ_{cu} by short, randomly oriented and located fibers has been derived by Li and Leung [4] for RSFRCCs with fiber pull-out:

$$\sigma_{cu}=g\sigma_0 \qquad (2)$$

Eqn. (2) was originated from relationship between composite crack bridging stress σ_c and crack opening displacement (COD) δ. This $\sigma_c-\delta$ relation is often referred as "bridging law" and depicted in Fig. 1, in which σ_{cu} was expressed as the stress at the peak point. In Eqn. (2), "g" indicates the stress increasing effect of fiber inclining angle, which was modeled as a rope passing over an Euler's friction pulley [11]. The FCS Criterion can then be written as:

$$\sigma_{fc}<\sigma_{cu} \qquad (3)$$

with σ_{fc} and σ_{cu} given by (1) and (2) respectively.

b) Steady State Cracking (SSC) Criterion

The phenomenon of steady state cracking in fiber reinforced brittle matrix composites has been studied by Aveston et al. [12], Marshall et al. [6 and 13], Li and Leung [4], Li [3], and Leung [7]. When steady state cracking occurs, a matrix crack will propagate steadily at essentially constant external tensile load (equal to the bridging stress of the fibers in an enlarging portion of the matrix crack) and at essentially constant crack opening except near the tip region. The presence or absence of this flat crack is dictated by energy balance between that absorbed at the propagating matrix crack tip, and the energy exchange between materials far ahead and far behind the crack tip (Marshall and Cox [6], Li [3], and Leung [7]). This energy balance consideration provides an estimation of the steady state stress σ_{ss} via the next formula.

$$J_{tip}=\sigma_{ss}\delta_{ss}-\int_0^{\delta_{ss}}\sigma_c(\delta)d\delta \qquad (4)$$

where,

σ_{ss}=Steady state cracking stress

δ_{ss}=COD corresponding to σ_{ss} in $\sigma_c-\delta$ curve

J_{tip}=Crack tip toughness

Since this steady state stress is physically limited to less than the maximum fiber bridging stress, or

$$\sigma_{ss}<\sigma_{cu} \qquad (5)$$

Eqn. (4) implies the SSC criterion

$$J_{tip}<J'_b \qquad (6)$$

where the complementary bridging energy J'_b is defined as

$$J'_b=\sigma_{cu}\delta_{cu}-\int_0^{\delta_{cu}}\sigma_c(\delta)d\delta \qquad (7)$$

where,

δ_{cu}=COD corresponding to σ_{cu}

J_{tip} and K_{tip} are related via

$$J_{tip}=\frac{K_{tip}^2}{E_c} \qquad (8)$$

Equation (6) together with (4) has a convenient interpretation (Marshall and Cox [6]) shown schematically in **Fig. 1**. J'_b and J_{tip} can be identified with the simply shaded and cross hatched areas in this figure. Equation (6) therefore places a limit on the matrix toughness. That is, the matrix toughness J_{tip} must be less than the comple-

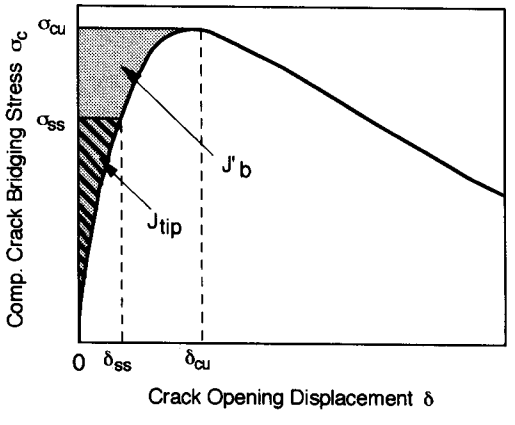

Fig. 1 Condition for steady-state cracking

mentary energy J'_b associated with the specifics of the bridging elements.

Satisfaction of the FCS Criterion (3) is not sufficient by itself for multiple cracking. Even when the first crack strength is low, as in the case of a composite containing a large flaw, energy balance required for steady state cracking may not be satisfied. When this occurs, the crack may extend with increasingly large crack opening in the mid-section of the crack so that fibers will either rupture or pull out, leaving only a near-tip section of the crack faces bridged.

Satisfaction of the SSC Criterion (6) by itself is also not sufficient for multiple cracking. The SSC Criterion does not place any restriction on matrix flaw size, so that for a composite which satisfies the SSC Criterion, it may have such small initial flaw sizes that the first crack stress exceeds the maximum bridging stress provided by the bridging fibers.

Thus, Eqns. (3) and (6) should be regarded as a pair of complementary criteria which must be simultaneously satisfied for multiple cracking to occur. Consideration of the above dual-criteria, together with the statistical nature of flaw size and fiber bridging properties, provides the foundation for understanding the sequential nature of multiple crack development and the saturation level of multiple cracks.

It should be noted that the adopted theories in this study are based on Linear Elastic Fracture Mechanics, in which inelastic deformation at matrix crack tip is expected to obey the small scale yielding condition. This means that relevant specimen size should be sufficiently larger than that of fracture process zone associated with the matrix crack extension process. The small scale yielding condition has been confirmed to be satisfied for cement paste or even mortar involving aggregate size less than 1 mm in specimens of a similar dimension as that used in the current study [5].

2.2 Theory for Crack Spacing

The crack spacing at ultimate tensile stress has been analytically derived for saturated PSH-RSFRCCs [2]:

$$x_d=\frac{L_f-\sqrt{L_f^2-2\pi\phi L_f x}}{2} \qquad (9)$$

where,

$\phi=\frac{4}{\pi g}$, $x=\frac{V_m\sigma_{mu}d_f}{4V_f\tau_i}$, σ_{mu}=Matrix crack stress

Eqn. (9) was derived by considering stress transfer from bridging fibers to matrix via interface friction in a cracked section. Prediction of crack spacing with Eqn. (9) is reported to be in agreement with observations in uniaxial tensile test data using Polyethylene PSH-RSFRCCs [2].

3. EXPERIMENT

This study employed uniaxial tensile tests in which the process of crack evolution and the development of crack opening displacement were observed. The experimental set-up is shown in **Fig. 2**. This test adopted specimens with a rather large section, 76 mm×38 mm, in order to reduce the effect of specimen section size on fiber alignment (L_f=19.1 mm). The overall uniaxial tensile strain was measured with 2 LVDTs, one on each side of the specimen. In addition, the realtime surface

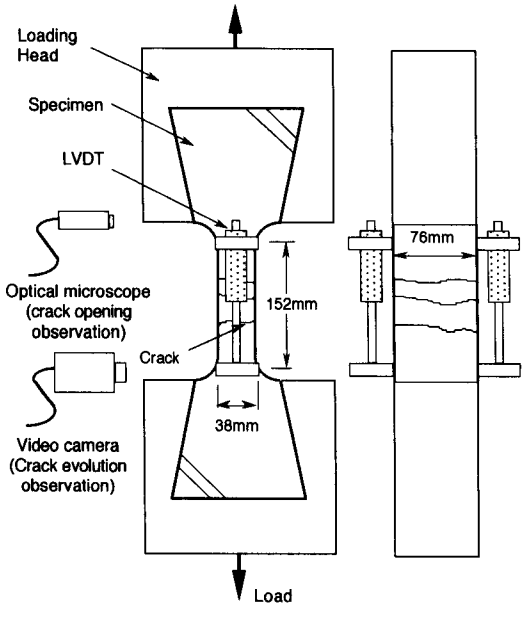

Fig. 2 Experimental set-up

Table 1 Mix proportion

W/C (%) (1)	Cement (2)	Silica fume (3)	water (4)	Super plasticizer (5)
*27	0.8	0.2	0.27	0.040

* Silica fume is included in cement weight

crack evolution (full-field) and COD development in the specimens were recorded with a video camera and an optical microscope (50 × magnification), respectively. Furthermore, the crack spacing and COD were closely examined after failure (specimens removed from load frame) by using the same optical microscope (post-mortem crack spacing examination, hereafter). The realtime crack evolution records reveal the time (load) and location of crack generation, useful for identification of the first, last and the failure cracks. The post-mortem crack spacing examinations were used to determine the saturation level of crack development by comparing the measured crack spacing with that estimated with Eqn. (9). Moreover, the post-mortem COD was examined to deduce the distribution of COD at ultimate strain $\varepsilon_{cu}{}^{test}$. Limited observations in the tests confirmed that crack closure was not significant after complete specimen unloading [2].

Raw materials and mix proportion (**Table 1**) were determined by referring to reference [2]. Composite constituent properties are summarized in **Table 2**. This experiment adopted a high modulus polyethylene fiber. The fiber volume fraction (0.5%, 0.75%, 1.0% and 1.25%) and fiber length (19.1 mm) falls within the range nominally satisfying PSH criteria (Eqns. (3) and (6)). Two specimens for every fiber volume fractions were tested at 4 week age. For the specimens with V_f=1.25%, tests were conducted at 1 week and 4 weeks.

The variation of V_f is meant to simulate variations in the fiber bridging properties, particularly the σ_{cu} and the J'_b discussed in Section 2. The test age variable is meant to roughly approximate the matrix toughness J_{tip}. The one week old specimens should have a lower J_{tip} than the four week old specimens, according to previous studies of age effect on toughness development of cementitious materials [14]. However, no direct measurement of the matrix toughness was performed in the present experimental series. The fiber/matrix

Table 2 Constituent properties of composites

Micromechanical parameter (1)	Polyethylene composite (2)
Matrix elastic modulus E_m (GPa)	23
Fiber elastic modulus E_f (GPa)	117
Nominal fiber strength $\sigma_{fu}{}^n$ (MPa)	2 400
Fiber volume fraction V_f (%)	0.5, 0.75, 1.0, 1.25
Friction bond strength τ_i (MPa)	0.62
Fiber length L_f (mm)	19.05
Fiber diameter d_f (mm)	0.038
Snubbing coefficient f	0.5

Table 3 Summary of tensile test results

Specimen		Test results					Estimated ultimate strain*1	Effective bond strength*2
Fiber volume fraction V_f (%) (1)	Curing age (week) (2)	First cracking stress $\sigma_{fc}{}^{test}$ (MPa) (3)	Ultimate strain $\varepsilon_{cu}{}^{test}$ (%) (4)	Ultimate stress $\sigma_{cu}{}^{test}$ (%) (5)	COD after loading $\delta_{cu}{}^{test}$ (μm) (6)	Crack space $x_d{}^{test}$ (mm) (7)	$\varepsilon_{cu}{}^{est}$ (%) (8)	(MPa) (9)
0.50	4	0.38 (0.39, 0.36)	0.73 (0.65, 0.80)	2.05 (1.95, 2.15)	–	–	–	1.09
0.75	4	2.27 (2.29, 2.26)	1.40 (1.30, 1.50)	2.49 (2.59, 2.39)	286 (250, 321)	19.2 (17.7, 20.6)	1.49	0.88
1.00	4	1.20 (1.21, 1.18)	3.80 (4.20, 3.40)	2.31 (2.43, 2.18)	217 (198, 236)	7.30 (5.25, 9.34)	3.16	0.61
1.25	4	1.68 (1.39, 1.96)	4.00 (3.90, 4.10)	2.74 (2.67, 2.81)	212 (190, 234)	4.83 (4.75, 4.90)	4.39	0.54
1.25	1	2.11 (2.36, 1.85)	7.25 (5.50, 9.0)	2.54 (2.61, 2.48)	208 (219, 198)	3.60 (4.83, 2.36)	6.35	0.58

Note : Test results are average of two specimens, and data for individual specimens are in parenthesis
*1 Using eqn. (10) *2 Inverted by using eqn. (2)

interface bond should also be expected to evolve with age. However, the bond property was found to mature at less than 7 days in several fiber types including the polyethylene fiber used in this test (Chan and Li [15]). Hence it is assumed that frictional bond strength τ_i is identical for the 1 week and 4 week specimens.

4. EXPERIMENTAL RESULT

4.1 Tensile Stress-Strain Relation

Except for the V_f=0.5%, all specimens showed PSH behavior while the intensity of PSH is different depending on V_f and age. Such behavior is illustrated in Fig. 3 (a) and (b), which show the stress-strain relationships obtained from the uniaxial tensile tests. Furthermore, important characteristics of the stress-strain relationships are summarized in **Table 3**. As shown in this table, test results are almost consistent between two specimens while data variability for ultimate strain and crack space is rather large for some composite types.

The stress-strain curves in Fig. 3 (a) and (b) show many sharp stress drops and subsequent recoveries. Ths sharp stress drops were observed to correspond to the generation of cracks. Therefore, the number of this stress fluctuation correlates with the number of multiple cracks. The number of the stress fluctuation is very different between specimens in **Fig. 3**. The specimen with V_f=0.5% shows smooth stressstrain curve which is attributed to single crack behavior while the specimen with V_f=1.25% showed numerous stress fluctuations, corresponding to the sequential development of multiple cracks. The PSH intensity can be represented by the ultimate strain ε_{cu}^{test}, defined as the strain when continuous stress drop occurs. ε_{cu}^{test} varies depending on V_f and age as shown in Table 3. This dependence is illustrated in **Fig. 4** which shows significant increase in ε_{cu}^{test} with V_f. For example, 4-week old composites with V_f =1.25% showed 4% of ε_{cu}^{test}, more than 5 times that of V_f=0.5% at the same age. Furthermore, the effect of age was remarkable on ε_{cu}^{test} which decreased from 7.25% to 4% between 1 week age and 4 week age.

It is expected that age should not have a significant influence on the ultimate strength of the composite, at least for those which undergoes pseudo strain-hardening. This is because for these com-

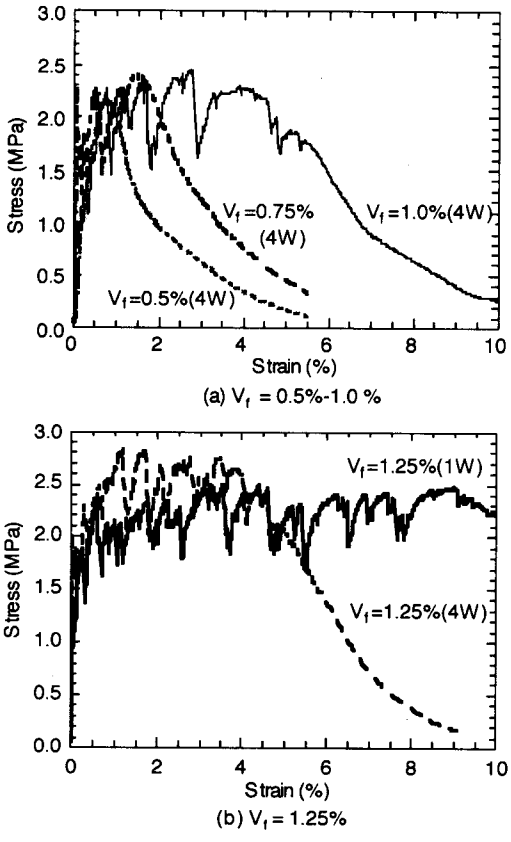

Fig. 3 Tensile stress-strain relations obtained in tests

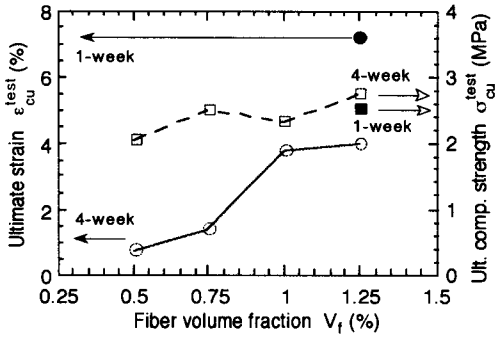

Fig. 4 Effects of fiber volume fraction and curing age on tensile strength and strain capacity.
○ for strain capacity, □ for ultimate strength, solid symbols for 1 week age, and open for 4 week age.

posites, the ultimate strength is in fact the maximum fiber bridging stress σ_{cu}. If, as argued above, the frictional bond does not change beyond 1 week age, then $\sigma_{cu}{}^{test}$, σ_{cu} observation in the tests, should also be unchanged. Table 3 or Fig. 4 confirms this expectation.

According to Eqn. (2), $\sigma_{cu}{}^{test}$ should scale linearly with V_f. However, Fig. 4 reveals that $\sigma_{cu}{}^{test}$ increases only by about 30% between V_f=0.5% and 1.25% at 4 week age. This result may be due to a deterioration of the apparent interfacial bond strength in composites with larger amount of fibers, perhaps associated with fiber-fiber interactions, e.g., fiber bundle formation, as have been reported in other studies (e.g., Li et al. [11]) An effective bond strength τ_{eff} can be identified from $\sigma_{cu}{}^{test}$ using Eqn. (2). τ_{eff} thus estimated decreases with V_f as shown in **Fig. 5**.

4.2 Experimental Observation of Crack Spacing and Crack Opening Displacement

Crack spacing and COD measured after unloading were intended to represent those when ultimate stress is attained in this study. Ignoring the small amount of elastic unloading, crack spacing is essentially constant after the ultimate strain $\varepsilon_{cu}{}^{test}$ is reached since crack generation is terminated after $\varepsilon_{cu}{}^{test}$. **Fig. 6** demonstrates that real-time measured COD is almost constant after $\varepsilon_{cu}{}^{test}$ is reached, for a limited test using a V_f=1.0% specimen. Similar to this result, slight crack closure (<10%) during unloading has been reported [2]. The post-mortem crack spacing and COD measured from a given specimen were averaged, and referred to as mean ultimate crack spacing

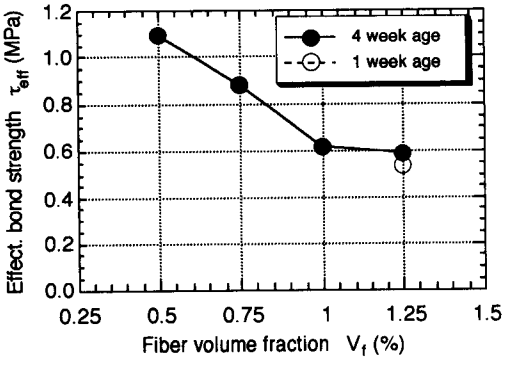

Fig. 5 Deduced effective bond strength

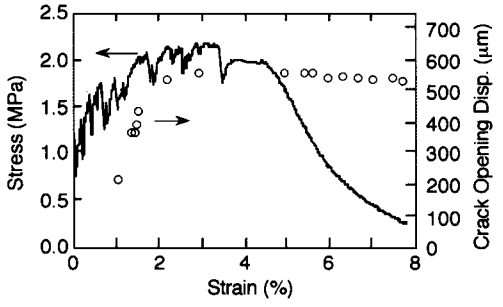

Fig. 6 Stress-strain relation and in-situ COD measure

$x_d{}^{test}$ and mean COD at ultimate stress, $\delta_{cu}{}^{test}$.

The strain capacity of PSH-RSFRRCs can be estimated from [16] :

$$\varepsilon_{cu}{}^{est}=\frac{\delta_{cu}{}^{test}}{x_d{}^{test}} \tag{10}$$

As shown in Table 3, evaluation of the right-hand side of Eqn. (10) gives estimated ultimate strain $\varepsilon_{cu}{}^{est}$ consistent with the directly measured $\varepsilon_{cu}{}^{test}$. This suggests that ε_{cu} can be predicted if x_d and δ_{cu} can be theoretically estimated.

The dependence of $x_d{}^{test}$ on V_f and age is depicted in **Fig. 7**, and that of $\delta_{cu}{}^{test}$ is shown in **Fig. 8**. Fig. 7 indicates that $x_d{}^{test}$ decreases significantly with V_f and age while Fig. 8 shows that $\delta_{cu}{}^{test}$ is relatively insensitive to these two parameters. Therefore, these tendencies imply that the influence of V_f and age on $\varepsilon_{cu}{}^{test}$ can be attributed to the difference in $x_d{}^{test}$ rather than that in $\delta_{cu}{}^{test}$. The calculated x_d (Eqn. (9)) for saturated PSH-RSFRCCs is also shown in Fig. 7. Although

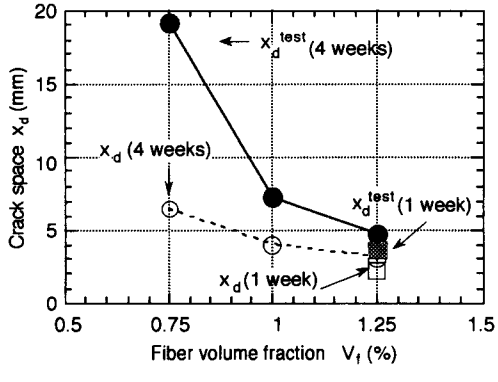

Fig. 7 Comparison of crack space between test (solid symbols) **and theory** (open symbols)

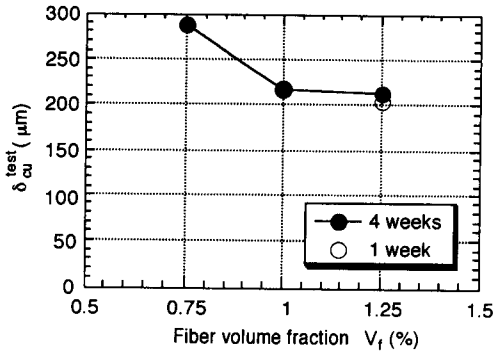

Fig. 8 COD at ultimate stress in test (δ_{cu}^{test})

reasonable for the V_f=1.25% case, the discrepancy between theory and experimental observation is large for the 0.75% and 1% cases, suggesting that these specimens do not have full saturation of multiple cracks. The lower sensitivity of δ_{cu}^{test} to V_f can be understood as a result of the cancellation effect between stiffer bridging elements (more fibers) and slightly higher load (σ_{cu}^{test}) at ultimate state for the larger V_f specimen. The suspected lower τ_{eff} (Fig. 5) with V_f should also lead to a reduced bridging stiffness. Recent theoretical consideration of δ_{cu} for composites [17] with interface slip-hardening behavior also suggests that δ_{cu} should be independent of V_f.

The distribution of crack spacing (Fig. 9) and COD (Fig. 10) is similar among specimens with no apparent dependence on either V_f or age. **Fig. 9** indicates that crack spacing appears skewed towards 3 mm or less. However, the actual computed average crack space x_d^{test} for specimens with lower V_f is much larger (Table 3 and Fig. 7). This is attributed to the fact that one order higher values of crack spacing, beyond the scale range in Fig. 9, are observed in specimens with lower V_f. These few data points of large crack spacing are responsible for the much higher average crack spacing for those specimens. Furthermore, **Fig. 10** depicts measured COD distribution skewed towards magnitude smaller than 200 μm. This dis-

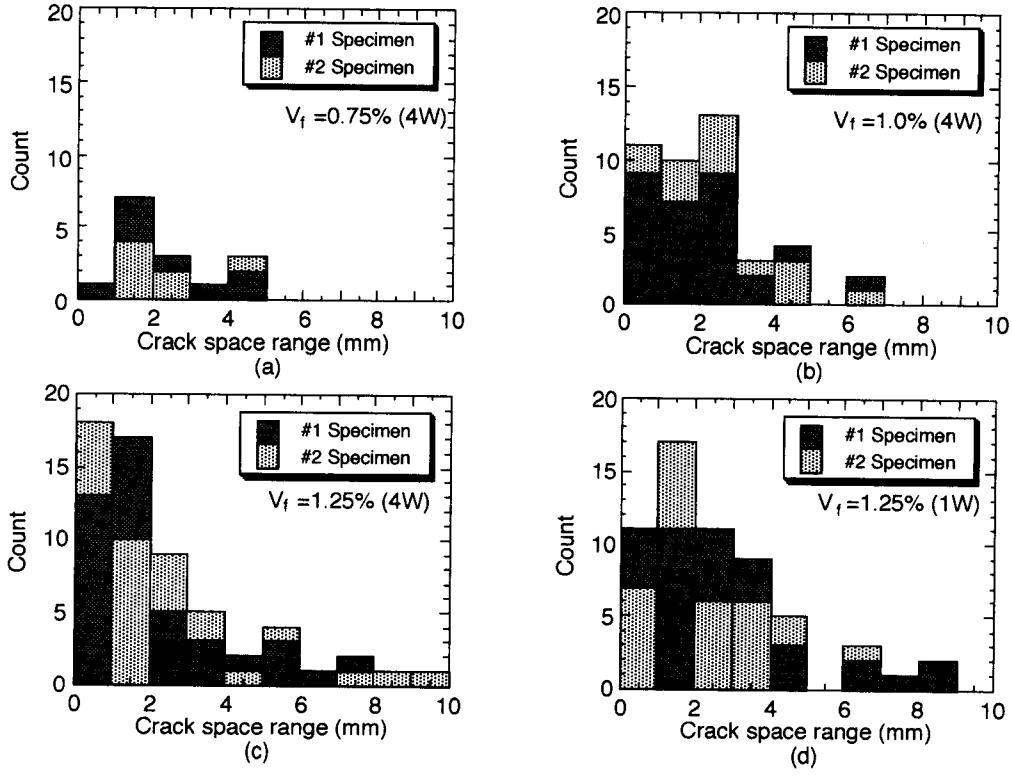

Fig. 9 Distribution of crack space for specimens (a) V_f=0.75%, 4 week age, (b) V_f=1.0%, 4 week age, (c) V_f=1.25%, 4 week age, and (d) V_f=1.25%, 1 week age

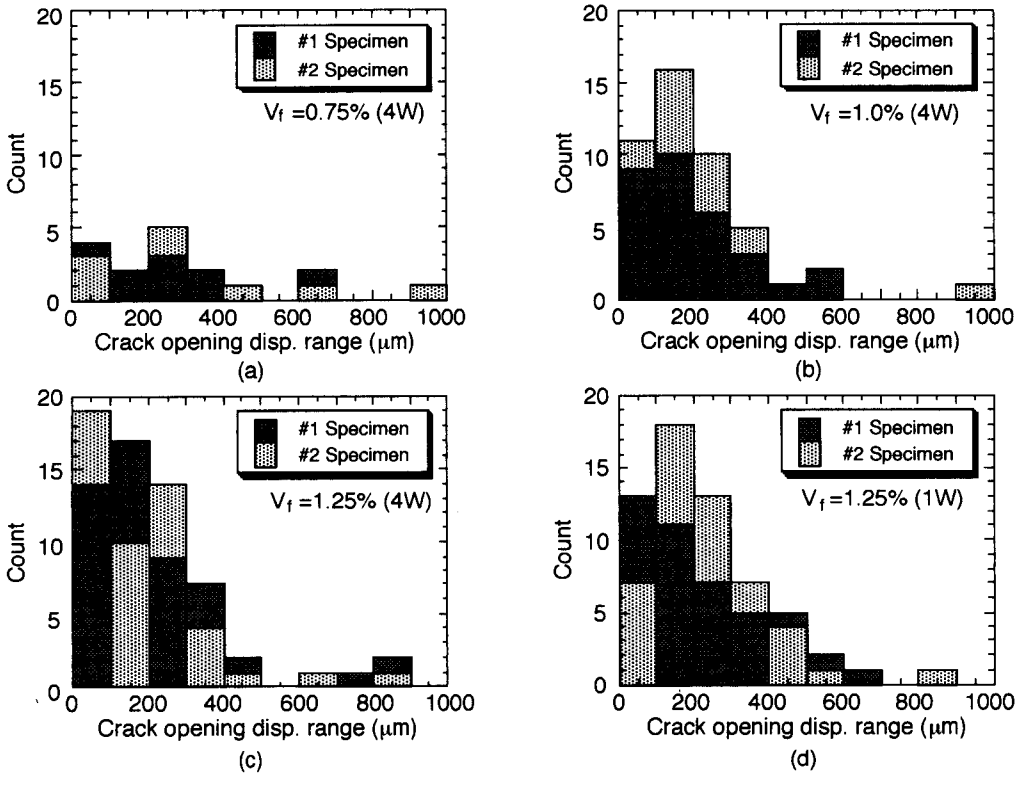

Fig. 10 Distribution of COD for specimens (a) V_f=0.75%, 4 week age, (b) V_f=1.0%, 4 week age, (c) V_f=1.25%, 4 week age, and (d) V_f=1.25%, 1 week age

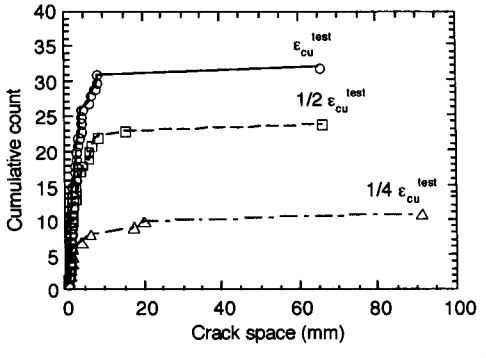

Fig. 11 Comparison of crack space distribution at different strain level (V_f=1.25% at 1 week age)

crepancy with the average COD reported in Table 3 is accredited to a couple of large COD data beyond 500 μm.

The saturation of crack development is depicted in **Fig. 11**, in which crack spacing distribution is compared at different strain levels, 0.25 ε_{cu}^{test}, 0.5 ε_{cu}^{test}, and ε_{cu}^{test}. This figure shows that the number of cracks significantly increases with the extent of applied composite strain. It implies that the increase of crack number is a major source of inelastic strain during the pseudo strain-hardening process. Furthermore, crack spacing distribution is shifted toward smaller magnitude of crack spacing with composite strain extent. This change in crack spacing distribution corresponds to the process of progressive crack saturation, in which cracks fill into virgin specimen sections as ε_{cu}^{test} is approached.

4.3 Observations of Crack Evolution

Three sequences of multiple crack evolution captured by video imaging are shown in Fig. 12 to 14. **Fig. 12** is for the specimen with V_f=1.25% tested at 1 week age. A band of multiple cracks seems to follow immediately after the appearance of the first crack (Fig. 12a). At a higher applied strain level (Fig. 12b), crack bands at other locations evolved. The failure crack in this specimen is also the last crack (Fig. 12c), and is not the same as

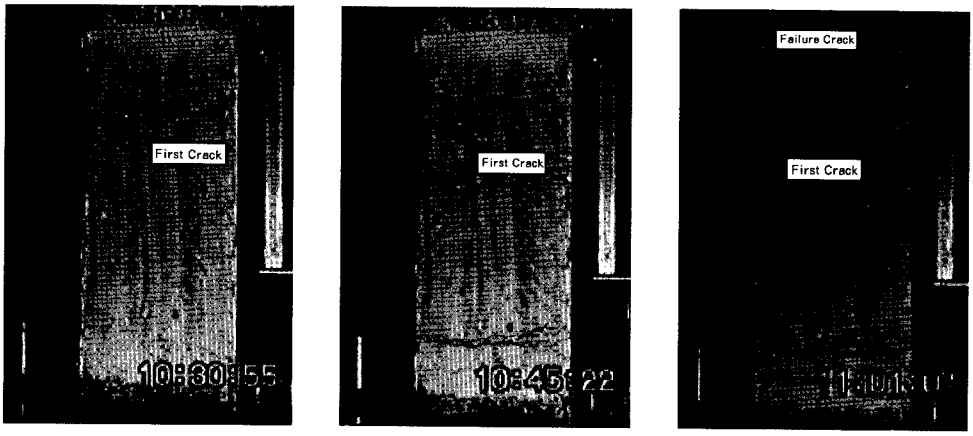

(a) at 0.05 ε_{cu} (b) at 0.57 ε_{cu} (c) after ε_{cu}

Fig. 12 The failure crack identical to the last crack (V_f=1.25% at 1 week age)

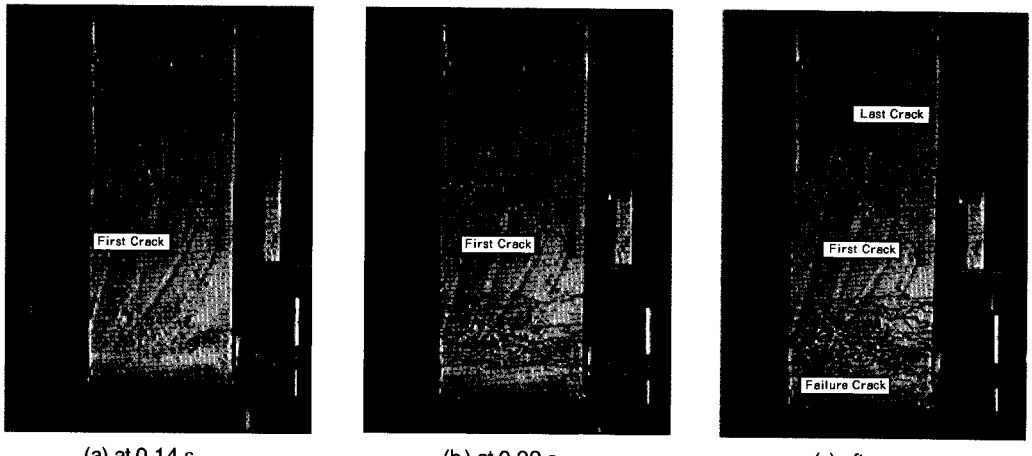

(a) at 0.14 ε_{cu} (b) at 0.92 ε_{cu} (c) after ε_{cu}

Fig. 13 The failure crack different from either the first or the last crack (V_f=1.0% at 4 week age)

the first crack. This particular specimen clearly demonstrates that the first crack need not be the failure crack at which deformation localization occurs and is accompanied by tension softening subsequently.

Fig. 13 shows the multiple crack evolution of the specimen with V_f=1.0% tested at 4 week age. The first crack (and crack band) is identified around the mid-section of the specimen in Fig. 13 (a). At higher applied strain level, a new band of cracks can be observed at the bottom end of the specimen (Fig. 13 b). Fig. 13 (c) shows further development of the original crack band above the first crack as loading is increased. Then the last crack indicated in Fig. 13 (c) occurred when ε_{cu} was almost at-

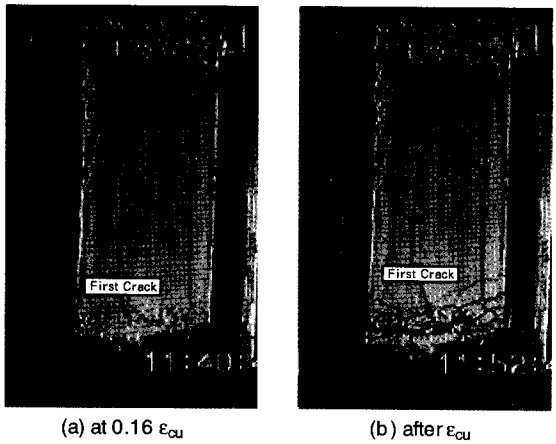

(a) at 0.16 ε_{cu} (b) after ε_{cu}

Fig. 14 The failure crack identical the first crack (V_f=0.75% at 4 week age)

tained. However, failure of the specimen did not occur at this location. Instead, it was observed that localization of deformation occurs among one of the cracks previously developed near the bottom of the specimen. This particular specimen illustrates that the failure crack also need not be identified with the last crack.

Fig. 14 shows the multiple crack evolution of the specimen with V_f=0.75% tested at 4 week age. In this case, only a single band of cracks developed and the failure crack is identical to be the first crack.

5. DISCUSSION

5.1 Three Possible Modes of Failure

The crack evolution processes described above, together with the theoretical background summarized in Section 2, suggest three scenarios for composites which develop unsaturated PSH. We begin this discussion by recognizing that RSFRCCs must have variations in initial matrix flaw size, and in fiber bridging properties. Variation in initial flaw size "c" may be a result of spatial variations in the compaction process, air void distribution and/or shrinkage crack formation (Hsu [18] and Kendall et al. [19]). Initial flaw size distribution will most likely influence the stress level to initiate the matrix crack. This implies that for a given specimen, larger cracks will be initiated first, while smaller cracks will be initiated as the tensile stress level increases during the pseudo strain-hardening process (if PSH occurs). The experimental observations of sequential development of multiple cracks at increasing applied load are consistent with this notion. It is also likely that matrix toughness K_m can fluctuate within a given specimen, although this may be difficult to measure directly. For each potential crack plane therefore, the "first" crack strength given by Eqn. (1) will be different depending on the magnitude of "c" and K_m. The experimental observation of better multiple crack saturation for the one week old specimen in comparison with the four week old specimen may be a result of the lower value of K_m at earlier age, which leads to better conformance to the FCS Criterion by Eqn. (3).

Fiber bridging properties in the form of J'_b or σ_{cu} also may fluctuate along the length of a specimen. Such fluctuations may be a result of variation in fiber volume fraction associated with non-uniform dispersion of fibers. For a crack plane with higher value of J'_b (or lower value of K_m or J_{tip}), improved conformance to the SSC Criterion (Eqn. (6)) is expected. The experimental observations of better saturation of multiple cracks in specimens with higher fiber volume fraction are consistent with this notion.

Suppose the first (n−1) cracks (or crack planes) in a specimen satisfy both the FCS and SSC Criteria, with $c_i < c_{i-1}$, such that $\sigma_{fc}{}^i > \sigma_{fc}{}^{i-1}$, following Eqn. (1). After the formation of these (n−1) multiple cracks, the n^{th} crack must have $c_n < c_i$; $\sigma_{fc}{}^n > \sigma_{fc}{}^i$ for i=1, …… n−1. In addition, for this n^{th} crack plane, it may have one of the following three characteristics:

(i) SSC satisfied
FCS not satisfied

(ii) FCS satisfied
SSC not satisfied

(iii) FCS satisfied
SSC satisfied
but $\sigma_{cu}{}^n < \sigma_{cu}{}^i$

For cases (i) or (ii), failure must occur immediately on this n^{th} crack plane. This means that the failure crack is also the last crack, as observed in the specimen discussed in connection with Fig. 12. For case (iii), continued multiple cracking can occur, but failure on this n^{th} crack plane will occur when the applied stress eventually reach $\sigma_{cu}{}^n$. In this case, the failure crack is obviously not the last crack. This corresponds to the case depicted in Fig. 13. In fact, if n=1, then the failure crack is identical to the first crack (corresponding to the case depicted in Fig. 14, but failure occurs only after some amount of multiple cracking).

The three scenarios (i)−(iii) represent some amount of 'short-coming' on the n^{th} crack plane, due to material variation in the specimen as discussed earlier in this section. This means that saturation of multiple cracking can be prematurely terminated, resulting in unsaturated PSH.

An exact prediction of the stress-strain curve of a PSH composite will require a full account of the

statistical distribution of matrix and crack bridging properties. However, this full account is beyond the scope in this study. At this stage, it may be realistic to suggest two indices based on the FCS and the SSC criteria as approximate measures of the tendency for multiple cracking saturation. This is discussed below.

5.2 PSH Indices

Finally, this study proposes to quantitatively represent the saturation of crack development by crack spacing ratio x_d^{test}/x_d and to correlate this ratio with two newly introduced micromechanical performance indices, J'_b/J_{tip} and σ_{cu}/σ_{fc}. J'_b, J_{tip}, σ_{cu}, and σ_{fc} can be calculated theoretically using Eqn. (1), (2), (7), and (8), respectively. These indices are prompted by the two PSH criteria Eqn. (3) and (6), and represent margins of criteria satisfaction. Materials with low margins (index values close to unity) can be expected to have little room for accommodating constituent property variation, thus leading to a higher tendency towards unsaturated PSH. It should be noted that calculating the second index σ_{cu}/σ_{fc} needs to identify critical initial flaw size responsible for first cracking. While this critical flaw size can be experimentally determined using special technique, flaw size investigation is beyond the scope of this study. Instead, the index $\sigma_{cu}^{test}/\sigma_{fc}^{test}$ is adopted, with σ_{fc}^{test} determined experimentally.

According to Aveston et al. [12], x_d^{test}/x_d should fall between 1 and 2 for saturated PSH behavior. Therefore, composites with x_d^{test}/x_d less than 2 may be classified as showing saturated PSH. In this study, composites with V_f more than 1% showed x_d^{test}/x_d less than 2, and this ratio tends to be reduced with increasing V_f. Fig. 15 illustrates the dependence of crack saturation x_d^{test}/x_d on energy margin J'_b/J_{tip}. The data point for specimens with V_f=0.5% was not included since these specimens showed single crack behavior which causes x_d^{test}/x_d tend to infinity. The upper limit of x_d^{test}/x_d=2 for full saturation [12] is also included as a reference value, and is shown with a horizontal broken line in **Fig. 15**. This level is attained when J'_b/J_{tip} exceeds about 3. Slightly larger critical margin J'_b/J_{tip}=4.0 was also deduced by the authors from a previous set of test

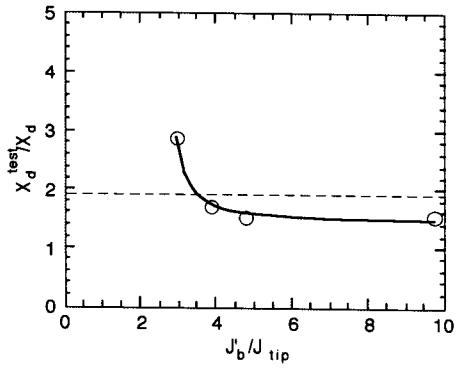

Fig. 15 Dependence of crack saturation on energy margin index

data [2]. Therefore, it may be concluded J'_b/J_{tip} >3 provides a reasonable basis for engineering judgment of saturated PSH potential.

The second performance index, $\sigma_{cu}^{test}/\sigma_{fc}^{test}$ can be interpreted as a measure of the size range of cracks which can be activated from the first crack stress associated with the largest flaw to the maximum bridging stress at which the composite fails. If this ratio is close to the lower bound of unity, one can expect fewer cracks to be initiated during the strain-hardening stage. Conversely, if this range is much larger than unity, cracks with a wider range of initial size should be included in the multiple cracking process. Ths effect of this stress or equivalently crack size margin on PSH saturation is illustrated in **Fig. 16**. This figure shows that x_d^{test}/x_d generally tends to decrease with increasing $\sigma_{cu}^{test}/\sigma_{fc}^{test}$ as expected. Using x_d^{test}/x_d=2 again as the reference line, the pre-

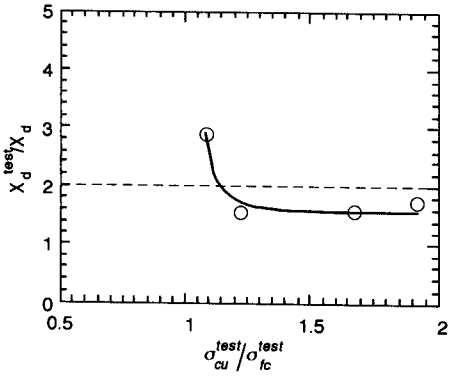

Fig. 16 Dependence of crack saturation on stress margin index

sent set of experimental data suggests a minimum value of this performance index of 1.2 for PSH saturation. This magnitude is also confirmed convincingly by using the test results of Wu and Li [2].

Achieving PSH behavior depends on both energy performance and strength performance of composites, represented by J'_b/J_{tip} and σ_{cu}/σ_{fc} respectively, for which the empirical lower bounds of 3.0 and 1.2 are suggested respectively. Clearly, the V_f =1.25% polyethylene fiber composites in the present series of tests meet these limits simultaneously, and they show saturated PSH behavior. In contrast, Nylon RSFRCCs tend to have low peak bridging stress as reported by Wu et al. [20]. This will likely violate the FCS criterion. Indeed σ_{cu}/σ_{fc} is estimated as 0.7 from the stress-strain curves reported in the same reference [20] while J'_b/J_{tip} evaluated by the authors attains surprisingly high magnitude exceeding 25. This estimation result is likely supported by uniaxial tensile test results for Nylon-RSFRCC in the reference [20], in which the tensile stress never fully recovered after the first cracking. This low value of σ_{cu}/σ_{fc} is attributed to substantially low frictional bond strength (0.15 MPa) in fiber/matrix interface for Nylon and obviously violates the required minimum of 1.2. This violation may be why no Nylon PSH-RSFRCC has been reported so far. Furthermore, while some RSFRCCs with high performance PVA fiber (14 μm diameter) have been reported [21] to show higher bridging strength than the Polyethylene composites used in this study, these PVA composites did not show clear PSH behavior. This is likely due to the low value of the J'_b/J_{tip} index, around unity, estimated based on experimental data in reference [21], even though this composite is considered to have high magnitude of σ_{cu}/σ_{fc} at least similar to the Polyethylene composites with saturated PSH investigated in the current study. The low value of the J'_b/J_{tip} index is due to the low complementary bridging energy resulting from strong chemical bonding of the PVA fibers in cementitious matrices. These examples illustrate that simultaneously meeting the lower bound limits of both energy and strength performance indices is critical to achieve saturated PSH behavior.

It should be noted that the proposed empirical lower bounds for J'_b/J_{tip} and σ_{cu}/σ_{fc} are likely influenced by material and processing details, and should therefore be regarded as approximate guidelines only. However, this study demonstrated that PSH composites should have certain margin in performances represented by the proposed two indices and that identical lower bounds for these indices may be employed for similar composites but with different testing age as well as different fiber volume content.

6. CONCLUSION

This study has focused on clarifying the sequence and saturation of multiple cracking evolution in PSH-RSFRCCs. Several specially designed PSH-RSFRCCs were examined through uniaxial tensile tests, in which the process of crack evolution and crack opening development were monitored. From the results of these experiments, it can be concluded that composites which nominally satisfy the FCS and SCC criteria do not necessarily show saturated PSH behavior. This discrepancy is attributed to the variability of micromechanical properties, specifically the matrix toughness, initial flaw size and fiber volume fraction.

The experimental observations of the first crack, the last crack, and the failure crack support the hypothesis of material constituent variability in a given specimen. Consideration of the FCS and SSC criteria suggests three possible modes of failure. All three modes were directly observed in this series of tests. It is concluded that the concepts behind the FCS and SSC criteria are sound, but should be extended to acoount for material constituent variability in order to access the extend of PSH. Finally, two micromechanics based performance indices, J'_b/J_{tip} and σ_{cu}/σ_{fc}, are proposed as measures of the potency for reaching PSH saturation in the face of material constituent variations, which are likely difficult to be completely eliminated in practice. Examination of the experimental results indicated that $J'_b/J_{tip}>3$ and $\sigma_{cu}/\sigma_{fc}>$ 1.2 may be necessary to secure saturated PSH behavior.

The effectiveness of the performance indices to delineate saturated PSH has been confirmed to be valid employing limited test data, in which composites are similar in fundamental configurations, e.g., with the same (polyethylene) fiber type and matrix mix proportion but different in fiber volume fraction and testing age. Their applicability and the specific limits derived from the present data set, to describe PSH saturation intensity of general composite systems, however, will require more extensive subsequent studies with a wider range of fiber and matrix types.

Acknowledgments

This work has been partially supported by a grant (NSF-G-CMS-9601262) from the National Science Foundation to the University of Michigan. This work was completed while V. Li was a Visiting Professor at the University of Tokyo, Japan.

Reference

1) Li, V.C. and Wu, H.C. : Conditions for Pseudo Strain-hardening in fiber reinforced brittle matrix composites, Appl. Mech. Review, Vol. 45, No. 8, pp. 390-398, 1992
2) Wu, H.C. and Li, V.C. : Stochastic Process of Multiple Cracking in Discontinuous Random fiber Reinforced Brittle Matrix Composites, Int'l J. of Damage Mechanics, Vol. 4, No. 1, pp. 83-102, 1995
3) Li, V.C. : From Micromechanics to Structural Engineering -The Design of Cementitious Composites for Civil Engineering Applications, J. Struct. Mech. Earthquake Eng., Japan Society of Civil Engineers, Vol. 10, No. 2, pp. 37-48, July, 1993
4) Li, V.C. and Leung, K.Y. : Steady-state and Multiple Cracking of Short Random Fiber Composites, Journal of Engineering Mechanics, ASCE, Vol. 118, No. 11, Nov., 1992
5) Li, V.C.; Mishra, D.K. and Wu, H.C. : Matrix Design for Pseudo-Strain -Hardening Fiber Reinforced Cementitious Composites, Materials and Structures, RILEM, Vol. 28, pp. 586-595, 1995
6) Marshall, D.B. and Cox, B.N. : A J-Integral Method for Calculating Steady-State Matrix Cracking Stresses in Composites, Mechanics of Materials Vol. 7, pp. 127-133, 1988
7) Leung, C.K. : Design Criteria for Pseudoductile Fiber-Reinforced Composites, J. of Engineering Mechanics, ASCE, Vol. 122, No. 1, pp. 10-18, 1996
8) Maalej, M. and Li, V.C. : Introduction of Strain Hardening Engineered Cementitious Composites in the Design of Reinforced Concrete Flexural Members for Improved Durability, American Concrete Institute Structural J.,Vol. 92, No. 2, pp. 167-176, March-April, 1995
9) Mishra, D.K. and Li, V.C. : Performance of a Ductile Plastic Hinge Designed with an Engineered Cementitious Composite, UMCEE Report No. 95-06, University of Michigan, February, 1995
10) Kanda, T. ; Wu, H.C. and Li, V.C. : New Theory for Predicting First Cracking of Random Short Fiber Reinforced Cementitious Composites, (in preparation), 1998
11) Li, V.C. ; Wang, Y and Backer, S. : Effect of Inclining Angle, Bundling, and Surface Treatment on Synthetic Fiber Pull-out from a Cement Matrix, Composites, Vol. 21, No. 2, pp. 132-140, 1990
12) Aveston, J. ; Cooper, G.A. and Kelly, A. : Single and Multiple Fracture, The Properties of Fiber Composites, IPC Science and Technology Press, Guildford, UK, pp. 15-26, 1971
13) Marshall, D.B. ; Cox, B.N. and Evans, A.G. : The Mechanics of Matrix Crackingl in Brittle-Matrix Fiber Composites, Acta Metallurgica, Vol. 33, No. 11, pp. 2013-2021, 1985
14) Ogishi, S. and Ono, H. : Effects of Experimental Parameters on Fracture Toughness of Cement Paste and Mortar, Japan Concrete Institute, Concrete Journal, Vol. 25, No. 2, pp. 113-125 (in Japanese), 1987
15) Chan, Y.W. and Li, V.C. : Age Effect on the Characteristics of Fiber/Cement Interfacial Bond, Journal of Materials Science Vol. 32, No. 19, pp. 5287-5292, 1997
16) Lin, Z. and Li, V.C. : Crack Bridging in Fiber Reinforced Cementitious Composites with Slip-Hardening Interface, J. Mechanics and Physics of Solids, Vol. 45, No. 5, pp. 763-787, 1997
17) Lin, Z., Kanda, T. and Li, V.C : On interface characterization and performance of fiberreinforced cementitious composites, Advanced Cement Based Materials (to be submitted), 1998
18) Hsu, T.T.C. : Mathematical Analysis of Shrinkage Stresses in a Model of Hardened Concrete, American Concrete Institute J., Vol. 60, No. 3, 1963
19) Kendall, K. ; Howard, A.J. and Birchall, J.D. : The Relation between Prosity, Microstructure and Strength, and the Approach to Advanced Cement-Based Materials, Phil. Trans. R. Soc. Lond., A 310, pp. 139-153, 1983
20) Wu, H.C. ; Matsumoto, T. and Li, V.C. : Buckling of Bridging Fibers in Composites, J. of Materials Science Letters Vol. 13, pp. 1800-1803, 1994
21) Kanda, T. and Li, V.C. : A New Micromechanics Design Theory for Pseudo Strain Hardening Cementitious Composite, Journal of Engineering Mechanics, ASCE (accepted for publication), 1998

(原稿受理年月日：1997年10月29日)

繊維補強セメント複合材料における複数クラックの生成過程と飽和について

閑田徹志・ビクター・C.・リー

Concrete Research and Technology, Vol. 9, No.2, July 1998

概　要：高靱性（疑似ひずみ硬化性）を示す短繊維補強セメント複合材料に生じる多数の平行クラック（複数クラック）の生成過程と飽和について明らかにするため，一軸引張試験を実施してマイクロメカニクスの観点から検討を行った。実験結果から，繊維混入量と試験材齢の違いによって，生じるクラック数の程度に差が生じ，クラックが材料表面を均等に覆う場合（飽和クラック）と偏在する場合とがあることがわかった（不飽和クラック）。本研究では，この違いが生じる機構を明らかにするとともに，クラック飽和の程度を予測するためマイクロメカニクスに基づく2つの性能指標を提案した。

キーワード：短繊維補強セメント複合材料，マイクロメカニクス，高靱性